

# Modeling of pseudo-acoustic P-waves in orthorhombic media with a lowrank approximation<sup>a</sup>

<sup>a</sup>Published in Geophysics, 78, no. 4, C33-C40, (2013)

*Xiaolei Song and Tariq Alkhalifah*

## ABSTRACT

Wavefield extrapolation in pseudo-acoustic orthorhombic anisotropic media suffers from wave-mode coupling and stability limitations in the parameter range. We use the dispersion relation for scalar wave propagation in pseudo-acoustic orthorhombic media to model acoustic wavefields. The wavenumber-domain application of the Laplacian operator allows us to propagate the P-waves exclusively, without imposing any conditions on the parameter range of stability. It also allows us to avoid dispersion artifacts commonly associated with evaluating the Laplacian operator in space domain using practical finite difference stencils. To handle the corresponding space-wavenumber mixed-domain operator, we apply the lowrank approximation approach. Considering the number of parameters necessary to describe orthorhombic anisotropy, the lowrank approach yields space-wavenumber decomposition of the extrapolator operator that is dependent on space location regardless of the parameters, a feature necessary for orthorhombic anisotropy. Numerical experiments show that the proposed wavefield extrapolator is accurate and practically free of dispersion. Furthermore, there is no coupling of qSv and qP waves, because we use the analytical dispersion solution corresponding to the *P*-wave.

## INTRODUCTION

Nowadays, a growing number of seismic modeling and imaging techniques are being developed to handle wave propagation in transversely isotropic media (TI). Such anisotropic phenomena are typical in sedimentary rocks, in which the process of lithification usually produces identifiable layering. In anisotropic media, the velocity is no longer described by a single parameter. Equations for anisotropic wave propagation are more complicated, even for simple cases. Although exact expressions for phase velocities in VTI media involve four independent parameters, It has been observed that only three parameters influence wave propagation and are of interest to surface seismic processing (Alkhalifah and Tsvankin, 1995). Different approximations have been developed to simplify anisotropic equations, such as the weak-anisotropy approximation (Thomsen, 1986), elliptical approximations (Helbig, 1983; Dellinger and

Muir, 1988), acoustic approximations (Alkhalifah, 1998, 2000) and anelliptic approximations (Dellinger et al., 1993; Muir, 1985; Fomel, 2004). Tectonic movement of the crust may rotate the rocks and tilt the natural vertical orientation of the symmetry axis (VTI), causing a tilted TI (TTI) anisotropy. In addition, tectonic stresses may also fracture rocks, inducing another TI with a symmetry axis parallel to the stress direction and usually normal to the sedimentation-based TI. The combination of these effects can be represented by an orthorhombic model with three mutually orthogonal planes of mirror symmetry; the P-waves in each symmetry plane can be described kinematically as an independent TI model. Realization of the importance of orthorhombic models mainly comes from observation of azimuthal velocity variations in flat-layered rocks, which may indicate valuable fracture properties of reservoirs (Tsvankin and Grechka, 2011).

Wavefields in anisotropic media are well described by the anisotropic elastic-wave equation. However, in practice, we often have little information about shear waves and prefer to deal with scalar wavefields, especially for conventional imaging of subsurface structure. Alkhalifah (2000) derived an acoustic scalar wave equation for VTI media by careful reparametrization followed by setting the shear velocity along the symmetry axis to zero, which provided accurate kinematics for the conventional elastic wavefield. Later on, Alkhalifah (2003) followed the same approach and introduced an acoustic wave equation of the sixth order in axis-aligned orthorhombic media. Fowler and King (2011) presented coupled systems of partial differential equations for pseudo-acoustic wave propagation in orthorhombic media by extending their previous work in TI media (Fowler et al., 2010). Zhang and Zhang (2011) extended self-adjoint differential operators in TTI media (Duvencek and Bakker, 2011; Zhang et al., 2011) to orthorhombic media.

Pseudo-acoustic P-wave modeling with coupled equations may have shear-wave numerical artifacts in the simulated wavefield (Grechka et al., 2004; Zhang et al., 2009; Duvencek et al., 2008). Those artifacts as well as sharp changes in symmetry axis tilting may introduce severe numerical dispersion and instability in modeling. Yoon et al. (2010) proposed to reduce the instability by making  $\epsilon = \delta$  in regions with rapid tilt changes. Fletcher et al. (2009) suggested that including a finite shear-wave velocity enhances the stability when solving the coupled equations. These methods can alleviate the instability problem; however, they may alter the wave propagation kinematics or still leave shear-wave components in the P-wave simulation. Shear-wave artifacts can be removed from the P-wavefield in the phase-shift extrapolation method because the P- and S-wave solutions lie in a different part of the wavenumber spectrum (Bale, 2007). A number of spectral methods are proposed to provide solutions which can completely avoid the shear-wave artifacts (Etgen and Brandsberg-Dahl, 2009; Song and Fomel, 2011; Fomel et al., 2012; Song et al., 2013; Chu and Stoffa, 2011; Zhan et al., 2012; Fowler and Lapilli, 2012).

In this paper, we adopt a dispersion relation for orthorhombic anisotropic media

(Alkhalifah, 2003) and introduce a mixed-domain acoustic wave extrapolator for time marching in orthorhombic media. We use the lowrank approximation (Fomel et al., 2010, 2012) to handle this mixed-domain operator. We demonstrate by numerical examples that our method is kinematically accurate. Furthermore, there is no coupling of quasi-P and quasi-SV waves in the wavefield and no constraints on Thomsen's parameters required for stability.

## THEORY

### Acoustic Wave Extrapolation

The acoustic wave equation is widely used in forward seismic modeling and reverse-time migration (Bednar, 2005; Etgen et al., 2009):

$$\frac{\partial^2 p}{\partial t^2} = v(\mathbf{x})^2 \nabla^2 p, \quad (1)$$

where  $p(\mathbf{x}, t)$  is the seismic pressure wavefield and  $v(\mathbf{x})$  is the wave propagation velocity.

Assuming the model is homogeneous  $v(\mathbf{x}) \equiv v_0$ , after a Fourier transform in space, we get the following explicit expression in the wavenumber domain:

$$\frac{d^2 \hat{p}}{dt^2} = -v_0^2 |\mathbf{k}|^2 \hat{p}, \quad (2)$$

where

$$\hat{p}(\mathbf{k}, t) = \int_{-\infty}^{+\infty} p(\mathbf{x}, t) e^{i\mathbf{k} \cdot \mathbf{x}} d\mathbf{x}. \quad (3)$$

Equation 2 has the following analytical solution:

$$\hat{p}(\mathbf{k}, t + \Delta t) = e^{\pm i|\mathbf{k}|v_0\Delta t} \hat{p}(\mathbf{k}, t), \quad (4)$$

which leads to the well-known second-order time-marching scheme (Etgen, 1989; Soubaras and Zhang, 2008):

$$p(\mathbf{x}, t + \Delta t) + p(\mathbf{x}, t - \Delta t) = 2 \int_{-\infty}^{+\infty} \hat{p}(\mathbf{k}, t) \cos(|\mathbf{k}|v_0\Delta t) e^{-i\mathbf{k} \cdot \mathbf{x}} d\mathbf{k}. \quad (5)$$

Equation 5 provides a very accurate and efficient solution in the case of a constant-velocity medium with the aid of FFTs. When the seismic wave velocity varies in the medium, equation 5 turns into a reasonable approximation by replacing  $v_0$  with  $v(\mathbf{x})$ ,

and taking small time steps,  $\Delta t$ . However, FFTs can no longer be applied directly to evaluate the inverse Fourier transform, because a space-wavenumber mixed-domain term appears in the integral operation:

$$W(\mathbf{x}, \mathbf{k}) = \cos(|\mathbf{k}|v(\mathbf{x})\Delta t). \quad (6)$$

As a result, a straightforward numerical implementation of wave extrapolation in a variable velocity medium with mixed-domain matrix 6 will increase the cost from  $O(N_x \log N_x)$  to  $O(N_x^2)$ , the original cost for the homogeneous case, in which  $N_x$  is the total size of the three-dimensional space grid. A number of numerical methods (Etgen and Brandsberg-Dahl, 2009; Liu et al., 2009; Zhang and Zhang, 2009; Du et al., 2010; Fomel et al., 2010, 2012; Song and Fomel, 2011; Song et al., 2011, 2013) have been proposed to overcome this mixed-domain problem.

In the case of orthorhombic acoustic modeling, we derive a new phase operator  $\phi(\mathbf{x}, \mathbf{k})$  to replace  $|\mathbf{k}|v(\mathbf{x})$  of the isotropic model. We describe the details in the next section.

## Dispersion Relation for Orthorhombic Anisotropic Media

In transversely isotropic (TI) media, the model is fully characterized by five elastic parameters and density. In orthorhombic media, nine elastic parameters and density are needed to describe the elastic model. The stiffness tensor  $c_{ijkl}$  for an orthorhombic model can be represented, using the compressed two-index Voigt notation, as follows:

$$\mathbf{C} = \begin{bmatrix} c_{11} & c_{12} & c_{13} & 0 & 0 & 0 \\ c_{12} & c_{22} & c_{23} & 0 & 0 & 0 \\ c_{13} & c_{23} & c_{33} & 0 & 0 & 0 \\ 0 & 0 & 0 & c_{44} & 0 & 0 \\ 0 & 0 & 0 & 0 & c_{55} & 0 \\ 0 & 0 & 0 & 0 & 0 & c_{66} \end{bmatrix}. \quad (7)$$

Instead of strictly adhering to the orthorhombic media used by Tsvankin (1997, 2005), Alkhalifah (2003) slightly changed the notations and used the following nine

parameters determined from the above stiffness tensor:

$$\begin{aligned}
v_v &= \sqrt{\frac{c_{33}}{\rho}} \\
v_{s1} &= \sqrt{\frac{c_{55}}{\rho}} \\
v_{s2} &= \sqrt{\frac{c_{44}}{\rho}} \\
v_{s3} &= \sqrt{\frac{c_{66}}{\rho}} \\
v_1 &= \sqrt{\frac{c_{13}(c_{13} + 2c_{55}) + c_{33}c_{55}}{\rho(c_{33} - c_{55})}} \\
v_2 &= \sqrt{\frac{c_{23}(c_{23} + 2c_{44}) + c_{33}c_{44}}{\rho(c_{33} - c_{44})}} \\
\eta_1 &= \frac{c_{11}(c_{33} - c_{55})}{2c_{13}(c_{13} + 2c_{55}) + 2c_{33}c_{55}} - \frac{1}{2} \\
\eta_2 &= \frac{c_{22}(c_{33} - c_{44})}{2c_{23}(c_{23} + 2c_{44}) + 2c_{33}c_{44}} - \frac{1}{2} \\
\delta &= \frac{(c_{12} + c_{66})^2 - (c_{11} - c_{66})^2}{2c_{11}(c_{11} - c_{66})},
\end{aligned} \tag{8}$$

where  $v_v$  is P-wave vertical phase velocity,  $v_{s1}$  and  $v_{s2}$  are S-wave vertical phase velocity polarized in the  $[x_2, x_3]$  and  $[x_1, x_3]$  planes,  $v_{s3}$  is S-wave horizontal phase velocity polarized in the  $[x_1, x_3]$  but propagating in the  $x_1$  direction,  $v_1$  and  $v_2$  are NMO P-wave velocities for horizontal reflectors in the  $[x_1, x_3]$  and  $[x_2, x_3]$  planes, and  $\eta_1$ ,  $\eta_2$ , and  $\delta$  are anisotropic parameters in the  $[x_1, x_3]$ ,  $[x_2, x_3]$ , and  $[x_1, x_2]$  planes.

The Christoffel equation in 3D anisotropic media takes the following general form (Chapman, 2004):

$$\Gamma_{ik}(x_s, \mathbf{p}) = a_{ijkl}(x_s)p_j p_l - \delta_{ik}, \tag{9}$$

with  $p_j = \frac{\partial \tau}{\partial x_j}$  and  $a_{ijkl} = \frac{c_{ijkl}}{\rho}$ , where  $p_j$  are components of the phase vector  $\mathbf{p}$ ,  $\tau$  is travel-time along the ray,  $\rho$  is density,  $x_s, s = 1, 2, 3$  are Cartesian coordinates for position along the ray, and  $\delta_{ik}$  is the Kronecker delta function.

Alkhalifah (1998) pointed out that setting the S-wave velocity to zero does not compromise accuracy in travelttime computations for TI media. This conclusion can be applied to orthorhombic media as well (Tsvankin, 1997). Alkhalifah (2003) showed that the kinematics of wave propagation is well described by acoustic approximation.

In orthorhombic media, the Christoffel equation 9 reduces to the following form if  $v_{s1}$ ,  $v_{s2}$ , and  $v_{s3}$  are set to zero:

$$\begin{bmatrix}
p_1^2 v_1^2 \xi_1 - 1 & \gamma p_1 p_2 v_1^2 \xi_1 & p_1 p_3 v_1 v_v \\
\gamma p_1 p_2 v_1^2 \xi_1 & p_2^2 v_2^2 \xi_2 - 1 & p_2 p_3 v_2 v_v \\
p_1 p_3 v_1 v_v & p_2 p_3 v_2 v_v & p_3^2 v_v^2 - 1
\end{bmatrix}, \tag{10}$$

where  $\gamma = \sqrt{1 + 2\delta}$ ,  $\xi_1 = 1 + 2\eta_1$  and  $\xi_2 = 1 + 2\eta_2$ .

We evaluate the determinant of matrix 10 and set it to zero. After replacing  $p_1$  with  $\frac{k_x}{\phi}$ ,  $p_2$  with  $\frac{k_y}{\phi}$ , and  $p_3$  with  $\frac{k_z}{\phi}$ , we obtain a cubic polynomial in  $\phi^2$  as follows:

$$\begin{aligned} & -\phi^6 + \phi^4 \left( 2v_1^2\eta_1 k_x^2 + v_1^2 k_x^2 + 2v_2^2\eta_2 k_y^2 + v_2^2 k_y^2 + v_v^2 k_z^2 \right) \\ & + \phi^2 \left( v_1^4 \gamma^2 \xi_1^2 k_x^2 k_y^2 - v_2^2 v_1^2 \xi_1 \xi_2 k_x^2 k_y^2 - 2v_v^2 v_1^2 \eta_1 k_x^2 k_z^2 \right. \\ & \left. - 2v_v^2 v_2^2 \eta_2 k_y^2 k_z^2 \right) - v_1^4 v_v^2 \gamma^2 \xi_1^2 k_x^2 k_y^2 k_z^2 + 2v_1^3 v_2 v_v^2 \gamma \xi_1 k_x^2 k_y^2 k_z^2 \\ & - v_1^2 v_2^2 v_v^2 (1 - 4\eta_1 \eta_2) k_x^2 k_y^2 k_z^2 = 0. \end{aligned} \quad (11)$$

One of the roots of the cubic polynomial corresponds to P-waves in acoustic media and is given by the following expression:

$$\phi^2 = \frac{1}{6} \left| -2^{2/3} d - \frac{2\sqrt[3]{2}(a^2 + 3b)}{d} + 2a \right|, \quad (12)$$

where

$$\begin{aligned} a &= 2v_1^2\eta_1 k_x^2 + v_1^2 k_x^2 + 2v_2^2\eta_2 k_y^2 + v_2^2 k_y^2 + v_v^2 k_z^2, \\ b &= v_1^4 k_x^2 k_y^2 (2\gamma\eta_1 + \gamma)^2 - v_2^2 v_1^2 (2\eta_1 + 1)(2\eta_2 + 1) k_x^2 k_y^2 \\ & \quad - 2v_v^2 v_1^2 \eta_1 k_x^2 k_z^2 - 2v_v^2 v_2^2 \eta_2 k_y^2 k_z^2, \\ c &= v_v^2 v_1^4 (-k_x^2) k_y^2 k_z^2 (2\gamma\eta_1 + \gamma)^2 + 2v_2 v_v^2 v_1^3 \gamma (2\eta_1 + 1) k_x^2 k_y^2 k_z^2 \\ & \quad - v_2^2 v_v^2 v_1^2 (1 - 4\eta_1 \eta_2) k_x^2 k_y^2 k_z^2, \\ d &= \sqrt[3]{-2a^3 + 3(e - 9c) - 9ab}, \\ e &= \sqrt{|-3b^2(a^2 + 4b) + 6ac(2a^2 + 9b) + 81c^2|}. \end{aligned}$$

This root reduces to the isotropic  $P$ -wave solution when we set  $v_1 = v_2 = v_3 = v$ ,  $\eta_1 = \eta_2 = 0$ , and  $\gamma = 1$ , in which  $\phi$  in expression 12 is then given by  $|\mathbf{k}|v$ , which is the same dispersion relation in isotropic media as that is shown in equation 6. In VTI media:  $v_1 = v_2 = v$ ,  $\eta_1 = \eta_2 = \eta$ , and  $\gamma = 1$ ,  $\phi$  in expression 12 reduces to

$$\phi(\mathbf{x}, \mathbf{k}) = \sqrt{\frac{1}{2}(v_h^2 k_h^2 + v_v^2 k_z^2) + \frac{1}{2}\sqrt{(v_h^2 k_h^2 + v_v^2 k_z^2)^2 - \frac{8\eta}{1+2\eta} v_h^2 v_v^2 k_h^2 k_z^2}}, \quad (13)$$

where  $v_h = v\sqrt{1+2\eta}$  is the  $P$ -wave phase velocity in the symmetry plane, and  $k_h = \sqrt{k_x^2 + k_y^2}$ . Expression 13 is the same as the dispersion relation for VTI media (Alkhalifah, 1998, 2000; Fomel, 2004).

## Tilted Orthorhombic Anisotropy

Tectonic movement of the crust may rotate the rocks and tilt the plane containing the vertical cracks, causing a tilted anisotropy. In the case of tilted orthorhombic media,  $k_x$ ,  $k_y$ , and  $k_z$  need to be replaced by  $\hat{k}_x$ ,  $\hat{k}_y$ , and  $\hat{k}_z$ , which are spatial wavenumbers evaluated in a rotated coordinate system aligned with the vectors normal to the orthorhombic symmetry planes:

$$\begin{aligned}\hat{k}_x &= k_x \cos \phi + k_y \sin \phi \\ \hat{k}_y &= -k_x \sin \phi \cos \theta + k_y \cos \phi \cos \theta + k_z \sin \theta \\ \hat{k}_z &= k_x \sin \phi \sin \theta - k_y \cos \phi \sin \theta + k_z \cos \theta,\end{aligned}\tag{14}$$

where  $\theta$  is the dip angle measured with respect to vertical and  $\phi$  is the azimuth angle, which is the angle between the original X-coordinate and the rotated one. The original vertical axis has the direction of  $\{\sin \theta \sin \phi, -\sin \theta \cos \phi, \cos \theta\}$ . For a more general rotation, one needs three angles to describe the transformation (Zhang and Zhang, 2011).

## LOWRANK APPROXIMATION

For orthorhombic media, the mixed-domain phase operator,  $\phi$ , is given by equation 12. Considering inhomogeneous media, we choose lowrank approximation (Fomel et al., 2010, 2012) to implement the mixed-domain operator.

Fomel et al. (2010, 2012) showed that mixed-domain matrix  $W(\mathbf{x}, \mathbf{k}) = \cos(\phi(\mathbf{x}, \mathbf{k})\Delta t)$ , which appears in wavefield extrapolation, can be decomposed using a separable representation:

$$W(\mathbf{x}, \mathbf{k}) \approx \sum_{m=1}^M \sum_{n=1}^N W(\mathbf{x}, \mathbf{k}_m) a_{mn} W(\mathbf{x}_n, \mathbf{k}).\tag{15}$$

$W(\mathbf{x}, \mathbf{k}_m)$  is a submatrix of  $W(\mathbf{x}, \mathbf{k})$  that consists of a few columns associated with  $\mathbf{k}_m$ ,  $W(\mathbf{x}_n, \mathbf{k})$  is another submatrix that contains some rows associated with  $\mathbf{x}_n$ , and  $a_{mn}$  stands for the coefficients. The construction of the separated form 15 follows the method of Engquist and Ying (2009). The main observation is that the columns of  $W(\mathbf{x}, \mathbf{k}_m)$  are able to span the column space of the original matrix and that the rows of  $W(\mathbf{x}_n, \mathbf{k})$  can span the row space as well as possible.

In the case of smooth models, the mixed-domain operator can be decomposed by a low-rank approximation. In models with serious roughness and randomness, the time step may be restricted to small values or otherwise; the rank will end up high. As a result, the computational cost maybe high.

To perform a linear-time lowrank decompositon as proposed by Fomel et al. (2012), we first need to restrict the mixed-domain  $\mathbf{W}$  to  $n$  randomly selected rows. In practice,  $n$  can be scaled as  $O(r \log N_x)$  and  $r$  is the numerical rank of  $\mathbf{W}$ . Then, we perform pivoted QR algorithm (Golub and Van Loan, 1996) to find the corresponding columns for  $W(\mathbf{x}, \mathbf{k}_m)$ . To find the rows for  $W(\mathbf{x}_n, \mathbf{k})$ , we apply the pivoted QR algorithm to  $\mathbf{W}^*$ .

Representation 15 speeds up the computation of  $p(\mathbf{x}, t + \Delta t)$  because

$$\begin{aligned} p(\mathbf{x}, t + \Delta t) + p(\mathbf{x}, t - \Delta t) &= 2 \int e^{-i\mathbf{x} \cdot \mathbf{k}} W(\mathbf{x}, \mathbf{k}) \hat{p}(\mathbf{k}, t) d\mathbf{k} \\ &\approx 2 \sum_{m=1}^M W(\mathbf{x}, \mathbf{k}_m) \left( \sum_{n=1}^N a_{mn} \left( \int e^{-i\mathbf{x}_n \cdot \mathbf{k}} W(\mathbf{x}_n, \mathbf{k}) \hat{p}(\mathbf{k}, t) d\mathbf{k} \right) \right). \end{aligned} \quad (16)$$

Evaluation of the last formula requires  $N$  inverse FFTs. Correspondingly, with lowrank approximation, the cost can be reduced to  $O(NN_x \log N_x)$ , where  $N_x$  is the model size and  $N$  is a small number, related to the rank of the above decomposition and it is automatically calculated for some given error level ( $10^{-5}$ ) with a pre-determined  $\Delta t$ .

Figure 1(a)-1(c) shows an orthorhombic model with smoothly varying velocity –  $v_1$ : 1500–3088 m/s,  $v_2$ : 1500–3686 m/s,  $v_v$ : 1500–3474 m/s,  $\eta_1 = 0.3$ ,  $\eta_2 = 0.1$ , and  $\gamma = 1.03$ . The time step  $\Delta t = 4ms$ . Figure 2 display error of lowrank decomposition for  $\cos(\phi\Delta t)$  at the location (-1.925 km, -1.925 km, -1.925 km) with relatively high velocity values,  $v_1 = 2.257$  km/s,  $v_2 = 2.534$  km/s,  $v_v = 2.438$  km/s. One can find the error level is around  $10^{-5}$ . Figure 3 display error of lowrank decomposition for  $\cos(\phi\Delta t)$  at the location (0.575 km, 0.575 km, 0.575 km) with relatively low velocity values,  $v_1 = 1.544$  km/s,  $v_2 = 1.561$  km/s,  $v_v = 1.554$  km/s. One can find the error is also well controlled.

We propose using the above lowrank approximation algorithm to handle mixed-domain operator  $\phi$  in equation 12 for wave extrapolation in orthorhombic media.

## NUMERICAL EXAMPLES

Figure 4(a)–4(c) shows wavefield snapshots (depth, inline, and crossline) in a vertical orthorhombic medium with constant parameters:  $v_v = 2km/s$ ,  $v_1 = 2.1km/s$ ,  $v_2 = 2.05km/s$ ,  $\eta_1 = 0.3$ ,  $\eta_2 = 0.1$ , and  $\gamma = 1$ . The time-step size is 1 ms and the space grid sizes in three directions are all 25 m. As the model is homogeneous, the rank is 1 for the lowrank decomposition. The depth slice is anelliptical, whereas the inline and crossline display different diamond shapes, indicating different VTI properties. In Figures 4(a)–4(c), red dashed lines are calculated using ray tracing. Note that the red dashed lines match the wavefront from the lowrank method very well.



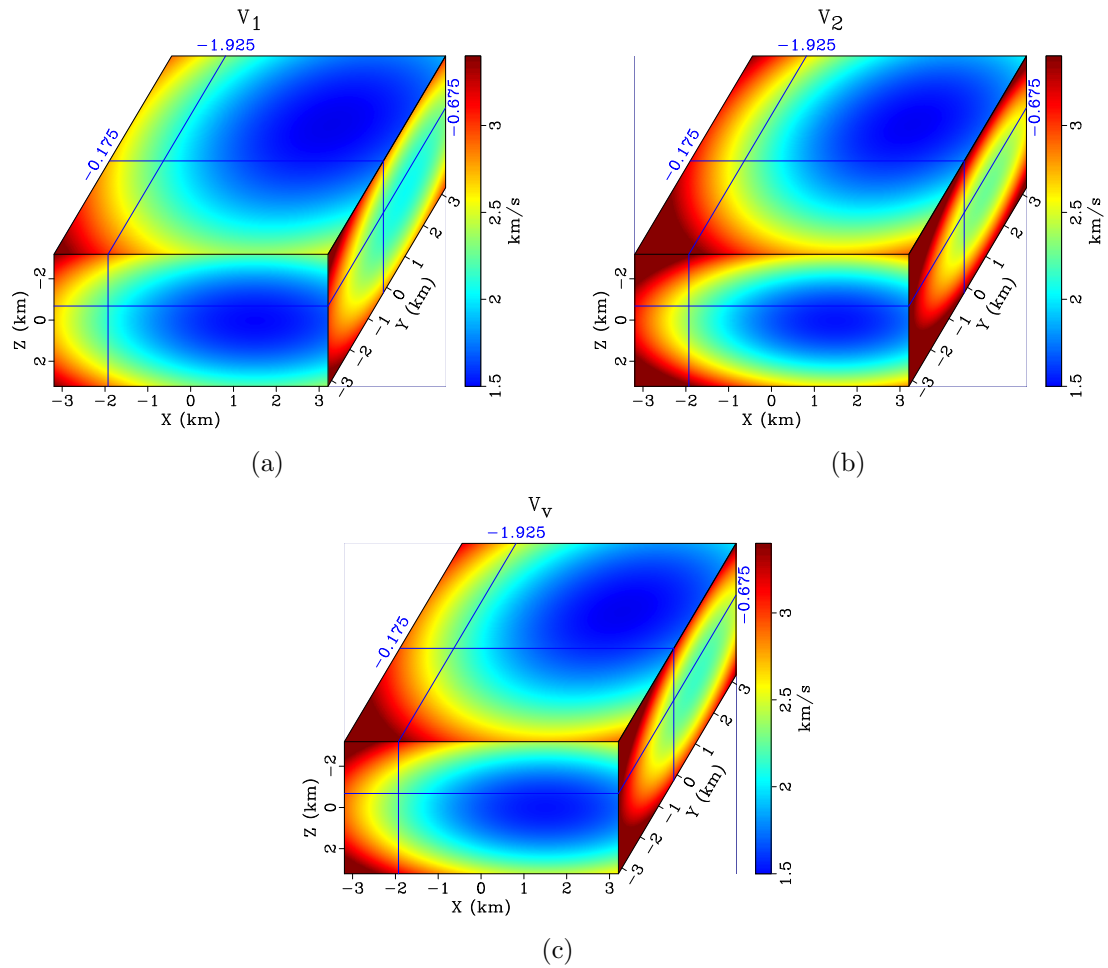


Figure 1: An orthorhombic model with smoothly varying velocity: (a)  $v_1$ : 1500–3088 m/s; (b)  $v_2$ : 1500–3686 m/s; (c)  $v_v$ : 1500–3474 m/s.

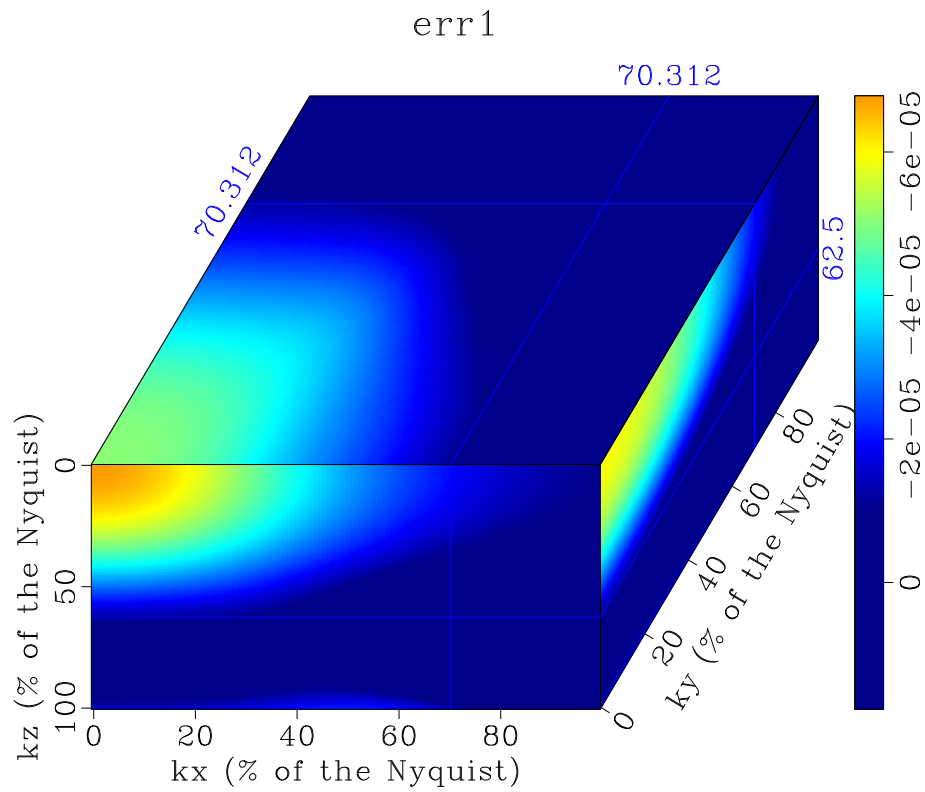


Figure 2: Error plot for the lowrank approximation for  $\cos(\phi\Delta t)$  at the location  $(-1.925 \text{ km}, -1.925 \text{ km}, -1.925 \text{ km})$  with relatively high velocity values,  $v_1 = 2.257 \text{ km/s}$ ,  $v_2 = 2.534 \text{ km/s}$ ,  $v_v = 2.438 \text{ km/s}$ .

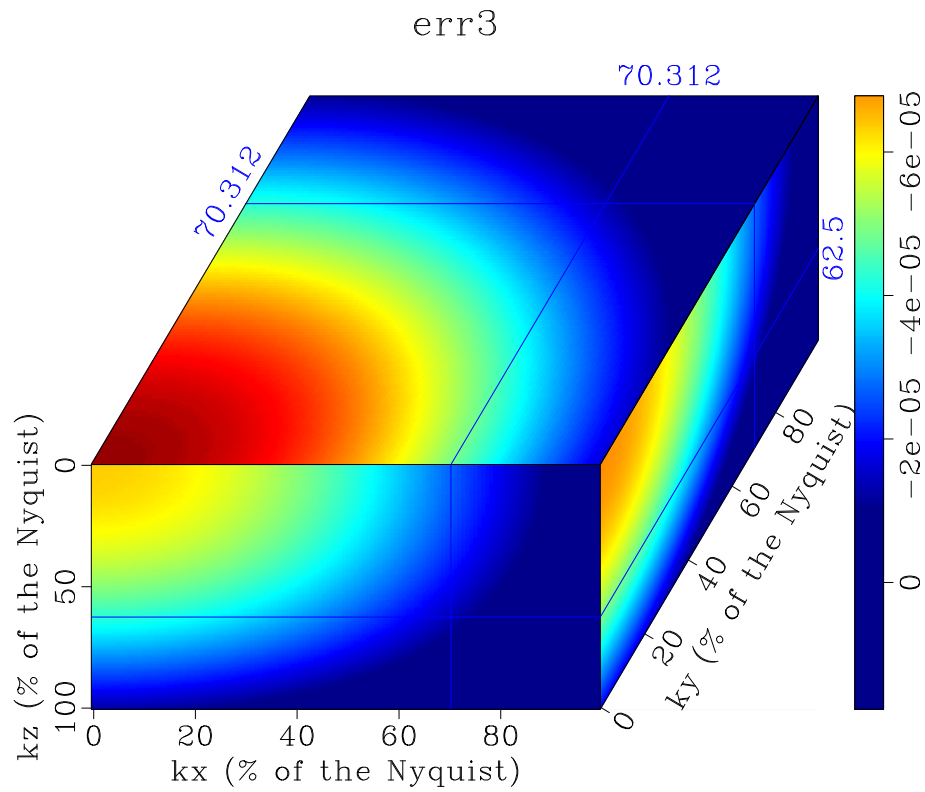


Figure 3: Error plot for the lowrank approximation for  $\cos(\phi\Delta t)$  at the location  $(0.575 \text{ km}, 0.575 \text{ km}, 0.575 \text{ km})$  with relatively low velocity values,  $v_1 = 1.544 \text{ km/s}$ ,  $v_2 = 1.561 \text{ km/s}$ ,  $v_v = 1.554 \text{ km/s}$ .

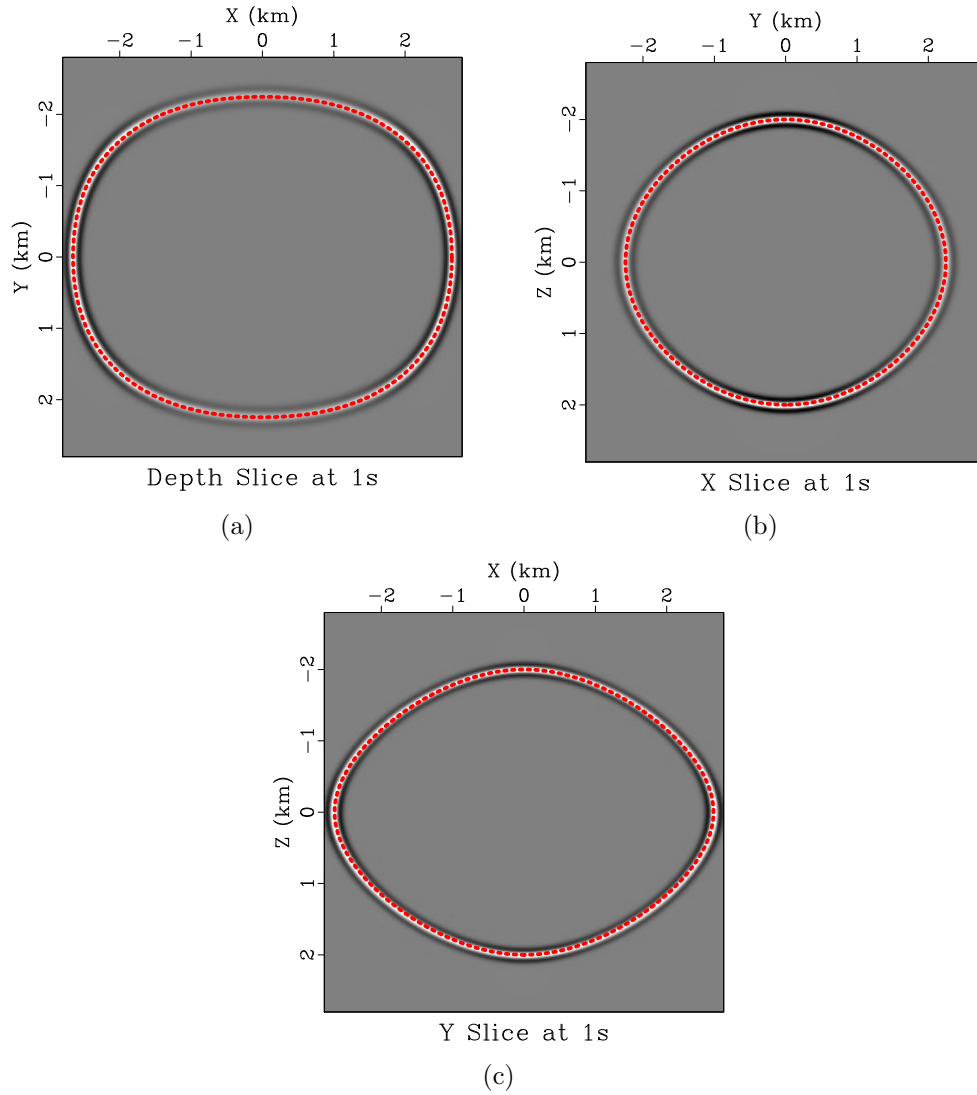


Figure 4: Three slices of the wavefield snapshot based on the dispersion relation 12 at 1 second in a vertical orthorhombic medium: (a) Depth Slice; (b) Inline Slice; (c) Crossline Slice. Also plotted are red curves representing the wavefront at that time calculated using raytracing.

To show that the lowrank approximation method can handle rough velocity models, we use a two-layer velocity model with high velocity contrast. The first layer has lower velocity parameters:  $v_v = 1.5\text{km/s}$ ,  $v_1 = 1.6\text{km/s}$ ,  $v_2 = 1.7\text{km/s}$ , while the values in the other layer are much higher:  $v_v = 3.5\text{km/s}$ ,  $v_1 = 4.1\text{km/s}$ ,  $v_2 = 4.2\text{km/s}$ . And we use the same anisotropic parameters for both layers:  $\eta_1 = 0.3$ ,  $\eta_2 = 0.1$ , and  $\gamma = 1$ . For this test, we use a time step size of 1 ms and a space grid size of 25 m. The rank is 2 calculated by the lowrank decomposition within an error level of  $10^{-5}$ . Figure 5(a) displays the depth slice above the reflector at 0.6 second. Note the snapshot shows the reflection from the velocity contrast. Figure 5(b) and 5(c) show the inline and crossline slices, which indicate strong anisotropy in the medium.

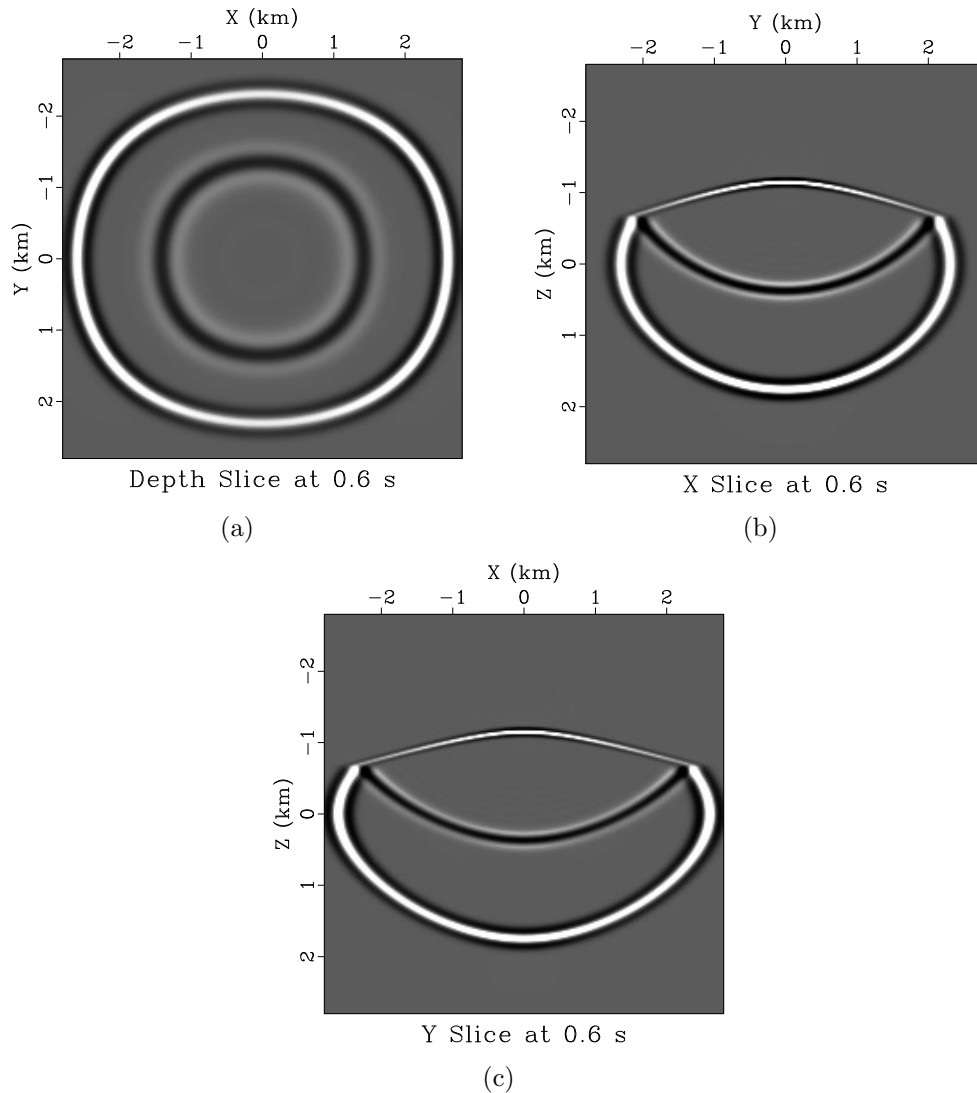


Figure 5: Three slices of the wavefield snapshot by the dispersion relation 12 at 0.6 second in a 2-layer vertical orthorhombic model (high velocity contrast): (a) Depth Slice; (b) Inline Slice; (c) Crossline Slice.

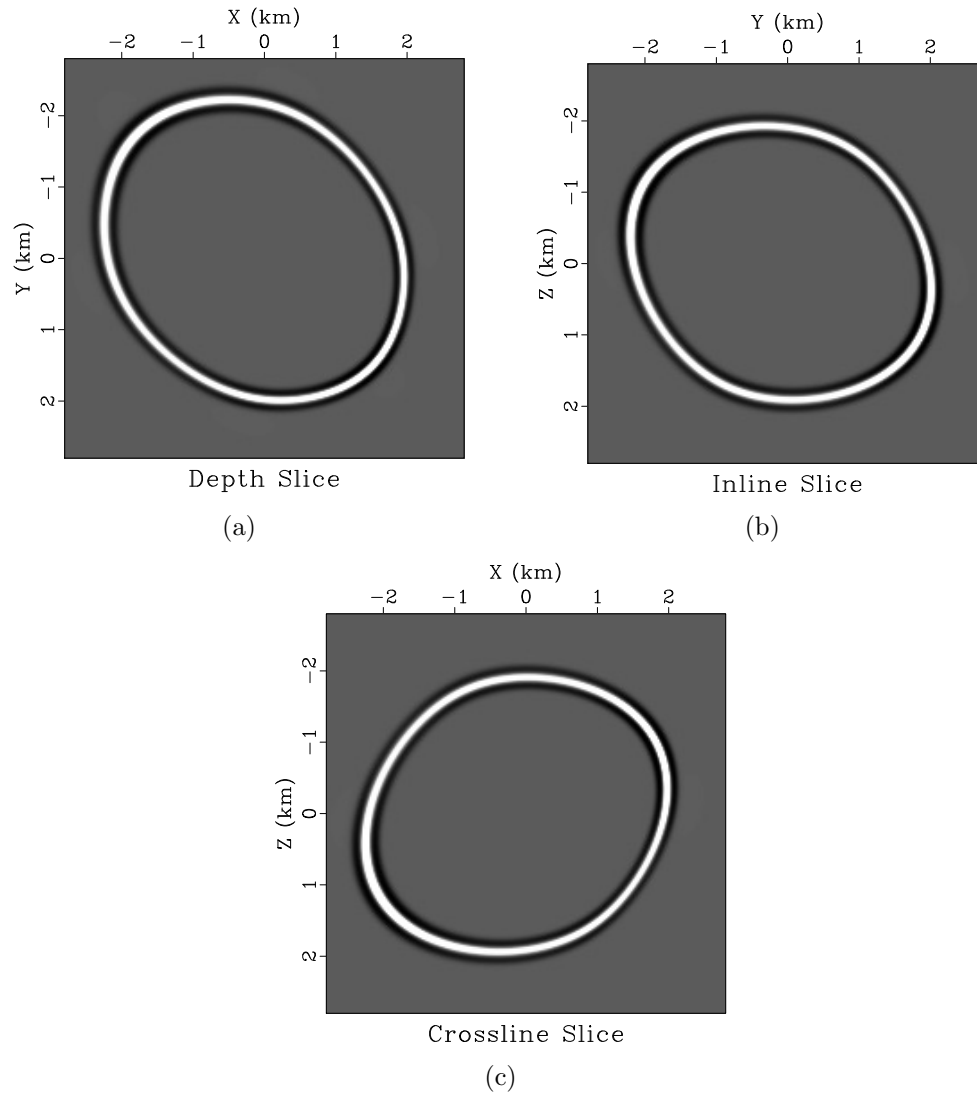


Figure 6: Wavefield snapshots based on the dispersion relation 12 in an rotated and tilted orthorhombic medium ( $\theta = \phi = 45^\circ$ ) with variable velocity shown in Figure 1(a)-1(c): (a) Depth Slice; (b) Inline Slice; (c) Crossline Slice

Our next example is wavefield snapshots in an orthorhombic model with smoothly varying velocity, shown in Figure 1(a)-1(c):  $v_1$ : 1500–3088 m/s,  $v_2$ : 1500–3686 m/s,  $v_v$ : 1500–3474 m/s,  $\eta_1 = 0.3$ ,  $\eta_2 = 0.1$ , and  $\gamma = 1.03$ . The time-step size is 4 ms. We also rotate the model ( $\theta = \phi = 45^\circ$ ). Figure 6(a)–6(c) shows corresponding wavefield snapshots by the dispersion relation 12 in depth, inline, and crossline slices through the central source location. The inline section (Figure 6(b)) displays the strongest anisotropic property, because  $\eta_1$  is as large as 0.3. Note that the snapshots are free of dispersion and that there is no coupling of qSV and qP waves in the middle. Lowrank parameters were  $M = 7$  and  $N = 7$ . Therefore, the cost is 7 FFTs at each time step.

Table 1 displays rank  $N$  required for maintaining an error level of  $10^{-5}$  with different time step size  $\Delta t$ . From table 1, one could find for this smooth model,  $\Delta t = 4$  ms and  $N = 7$  is the optimal choice for cost consideration. For models with very wide range of parameters and rather complicated structures, the resulting rank may be high, because more space locations and wavenumbers are required to properly represent the original mixed-domain matrix. In order to reduce the computational cost, one may consider Lowrank Finite differences proposed by Song et al. (2013), which is a space-domain finite-difference scheme in which the coefficients of the Laplacian finite-difference stencil is derived from the lowrank approximation.

$\Delta t$ (ms)	0.5	1	2	3	4	5
Rank $N$	5	5	7	7	7	12

Table 1: Rank  $N$  calculated from the lowrank approximation of the propagation matrix for a 2D smooth orthorhombic model with different time step size  $\Delta t$  for a given error level  $10^{-5}$ .

## CONCLUSIONS

We derive and adopt a dispersion relation for acoustic orthorhombic media so as to model seismic wavefields in such media. To handle the space-wavenumber mixed-domain operator, we apply the lowrank approximation to reduce computational cost. Numerical experiments show that the proposed wavefield extrapolator is accurate. There is no coupling of qSV and qP in the wavefield snapshots because we use the dispersion relation. In addition, our approach yields practically dispersion-free wavefields, and it is also free of stability limitations on media parameters.

## ACKNOWLEDGMENTS

We thank Sergey Fomel and Lexing Ying for their help with the lowrank algorithm, and Mirko van der Baan, Richard Bale, Paul J. Fowler, Samuel Gray, and one anonymous reviewer for helpful reviews. We also thank KAUST (King Abdullah University

of Science and Technology) and TCCS (Texas Consortium for Computational Seismology) for financial support. This publication is authorized by the Director, Bureau of Economic Geology, The University of Texas at Austin.

## REFERENCES

- Alkhalifah, T., 1998, Acoustic approximations for processing in transversely isotropic media: *Geophysics*, **63**, 623–631.
- , 2000, An acoustic wave equation for anisotropic media: *Geophysics*, **65**, 1239–1250.
- , 2003, An acoustic wave equation for orthorhombic anisotropy: *Geophysics*, **68**, 1169–1172.
- Alkhalifah, T., and I. Tsvankin, 1995, Velocity analysis for transversely isotropic media: *Geophysics*, **60**, 1550–1566.
- Bale, R. A., 2007, Phase-shift migration and the anisotropic acoustic wave equation: 69th Annual EAGE Meeting, EAGE, Expanded Abstracts, C021.
- Bednar, J., 2005, A brief history of seismic migration: *Geophysics*, **70**, 3MJ–20MJ.
- Chapman, C., 2004, *Fundamentals of seismic wave propagation*: Cambridge University Press.
- Chu, C., and P. L. Stoffa, 2011, Application of normalized pseudo-Laplacian to elastic wave modeling on staggered grids: *Geophysics*, **76**, T113–T121.
- Dellinger, J., and F. Muir, 1988, Imaging reflections in elliptically anisotropic media: *Geophysics*, **53**, 1616–1618.
- Dellinger, J., F. Muir, and M. Karrenbach, 1993, Anelliptic approximations for TI media: *Jour. Seis. Expl.*, **2**, 23–40.
- Du, X., R. P. Fletcher, and P. J. Fowler, 2010, Pure P-wave propagators versus pseudo-acoustic propagators for RTM in VTI media: 72nd Annual EAGE Meeting, EAGE, Expanded Abstracts, C013.
- Duveneck, E., and P. M. Bakker, 2011, Stable P-wave modeling for reverse-time migration in tilted TI media: *Geophysics*, **76**, S65–S75.
- Duveneck, E., P. Milcik, P. M. Bakker, and C. Perkins, 2008, Acoustic VTI wave equations and their application for anisotropic reverse-time migration: 78th Ann. Internat. Mtg., Soc. Expl. Geophys., 2186–2190.
- Engquist, B., and L. Ying, 2009, A fast directional algorithm for high frequency acoustic scattering in two dimensions: *Commun. Math. Sci.*, **7**, 327–345.
- Etgen, J., 1989, Accurate wave equation modeling, *in* SEP-60: Stanford Exploration Project, 131–148.
- Etgen, J., and S. Brandsberg-Dahl, 2009, The pseudo-analytical method: application of pseudo-Laplacians to acoustic and acoustic anisotropic wave propagation: 79th Annual International Meeting, SEG, Expanded Abstracts, 2552–2556.
- Etgen, J., S. H. Gray, and Y. Zhang, 2009, An overview of depth imaging in exploration geophysics: *Geophysics*, **74**, WCA5–WCA17.
- Fletcher, R. P., X. Du, and P. J. Fowler, 2009, Reverse time migration in tilted transversely isotropic (TTI) media: *Geophysics*, **74**, WCA179–WCA187.



- Fomel, S., 2004, On anelliptic approximations for qP velocities in VTI media: *Geophysical Prospecting*, **52**, 247–259.
- Fomel, S., L. Ying, and X. Song, 2010, Seismic wave extrapolation using a lowrank symbol approximation: 80th Ann. Internat. Mtg., Soc. Expl. Geophys., 3092–3096.
- , 2012, Seismic wave extrapolation using lowrank symbol approximation: *Geophysical Prospecting*, doi: 10.1111/j.1365-2478.2012.01064.x.
- Fowler, P. J., X. Du, and R. P. Fletcher, 2010, Coupled equations for reverse time migration in transversely isotropic media: *Geophysics*, **75**, S11–S22.
- Fowler, P. J., and R. King, 2011, Modeling and reverse time migration of orthorhombic pseudo-acoustic P-waves: 81th Ann. Internat. Mtg., Soc. Expl. Geophys., 190–195.
- Fowler, P. J., and C. Lapilli, 2012, Generalized pseudospectral methods for modeling and reverse-time migration in orthorhombic media: 74th Annual EAGE Meeting, EAGE, Expanded Abstracts, AO22.
- Golub, G. H., and C. F. Van Loan, 1996, *Matrix computations*: John Hopkins.
- Grechka, V., L. Zhang, and J. W. Rector, 2004, Shear waves in acoustic anisotropic media: *Geophysics*, **69**, 576–582.
- Helbig, K., 1983, Elliptical anisotropy its significance and meaning: *Geophysics*, **48**, 825–832.
- Liu, F., S. A. Morton, S. Jiang, L. Ni, and J. P. Leveille, 2009, Decoupled wave equations for P and SV waves in an acoustic VTI media: 79th Ann. Internat. Mtg., Soc. Expl. Geophys., 2844–2848.
- Muir, F., 1985, A practical anisotropic system: SEP-44, 55–58.
- Song, X., and S. Fomel, 2011, Fourier finite-difference wave propagation: *Geophysics*, **76**, T123–T129.
- Song, X., S. Fomel, and L. Ying, 2013, Lowrank finite-differences and lowrank Fourier finite-differences for seismic wave extrapolation in the acoustic approximation: *Geophysical Journal International*, doi: 10.1093/gji/ggt017.
- Song, X., S. Fomel, L. Ying, and T. Ding, 2011, Lowrank finite-differences for wave extrapolation: 81th Ann. Internat. Mtg., Soc. Expl. Geophys., 3372–3376.
- Soubaras, R., and Y. Zhang, 2008, Two-step explicit marching method for reverse time migration: 78th Ann. Internat. Mtg., Soc. Expl. Geophys., 2272–2276.
- Thomsen, L., 1986, Weak elastic anisotropy: *Geophysics*, **51**, 1954–1966.
- Tsvankin, I., 1997, Anisotropic parameters and P-wave velocity for orthorhombic media: *Geophysics*, **62**, 1292–1309.
- , 2005, *Seismic signature and analysis of reflection data in anisotropic media*: Elsevier Science.
- Tsvankin, I., and V. Grechka, 2011, Seismology of azimuthally anisotropic media and seismic fracture characterization: *Society of Exploration Geophysicists*.
- Yoon, K., S. Suh, J. Ji, J. Cai, and B. Wang, 2010, Stability and speedup issues in TTI RTM implementation: 80th Ann. Internat. Mtg., Soc. Expl. Geophys., 3221–3225.
- Zhan, G., R. C. Pestana, and P. L. Stoffa, 2012, Decoupled equations for reverse time migration in tilted transversely isotropic media: *Geophysics*, **77**, T37–T45.
- Zhang, H., G. Zhang, and Y. Zhang, 2009, Removing s-wave noise in TTI reverse time migration: 79th Ann. Internat. Mtg., Soc. Expl. Geophys., 2849–2853.
- Zhang, H., and Y. Zhang, 2011, Reverse time migration in vertical and tilted or-

thorhombic media: 81th Ann. Internat. Mtg., Soc. Expl. Geophys., 185–189.

Zhang, Y., and G. Zhang, 2009, One-step extrapolation method for reverse time migration: *Geophysics*, **74**, A29–A33.

Zhang, Y., H. Zhang, and G. Zhang, 2011, A stable TTI reverse time migration and its implementation: *Geophysics*, **76**, WA3–WA9.